McCormick A, Donoghue P, Dixon M, O'Sullivan R, O'Donnell RL, Murray J, Kaufmann A, Curtin NJ, Edmondson RJ.

Ovarian Cancers Harbour Defects in Non-Homologous End Joining Resulting in Resistance to Rucaparib.

***Clinical Cancer Research* (2016)**

DOI: http://dx.doi.org/10.1158/1078-0432.CCR-16-0564

Title: Ovarian Cancers Harbour Defects in Non-Homologous End Joining Resulting in Resistance to Rucaparib

Authors: Aiste McCormick [a], Peter Donoghue [a], Michelle Dixon [a], Richard O'Sullivan [a], Rachel L O'Donnell [a,b], James Murray [a], Angelika Kaufmann[a,b], Nicola J Curtin[a*], Richard J Edmondson[c*]

[a]Northern Institute for Cancer Research, Newcastle University, Framlington Place, Newcastle upon Tyne, NE2 4AD

[b]Northern Gynaecological Oncology Centre, Queen Elizabeth Hospital, Gateshead, NE9 6SX

[c]Faculty Institute for Cancer Studies, University of Manchester, St Marys Hospital, Oxford Road, Manchester, M13 9WL

[*] joint corresponding authors

Running Title: Defective NHEJ function in ovarian cancer

Key words: Non-homologous end joining, homologous recombination, ovarian cancer, PARP inhibitors, rucaparib, cisplatin, DNA-PK, XRCC6 (Ku70), XRCC5 (Ku80)

Funding: This work was supported by Cancer Research UK. Grant number C27826/A12498.

Corresponding authors
RJ Edmondson
Chair of Gynaecological Oncology
Faculty Institute for Cancer Sciences,
University of Manchester,
Manchester Academic Health Science Centre,
St Mary's Hospital,
Research Floor (5),
Oxford Road,
Manchester,
M13 9WL, UK
richard.edmondson@manchester.ac.uk

NJ Curtin
Professor of Experimental Cancer Therapy
Newcastle University
Northern Institute for Cancer Research and Newcastle University Institute for Ageing
Paul O'Gorman Building
Medical School
Newcastle upon Tyne
NE2 4HH, UK
n.j.curtin@ncl.ac.uk

Conflicts of interest - Authors have no conflicts of interests to declare.

Word count (excluding references): 3632

Total number of figures and tables: 7 figures.

Supplementary figures – 1. Supplementary table - 1.

Statement of Translational Relevance

Here, we have shown that non homologous end joining is critically important in determining sensitivity to PARP inhibitors. 40% of ovarian cancers tested had defective NHEJ and this rendered them resistant to PARP inhibition, irrespective of their Homologous Recombination status.

To date, the priority for developing accurate biomarkers for PARP sensitivity has focussed on developing surrogate markers for HR status. This work suggests that this will not be enough and a more detailed assessment of the DNA damage response, including NHEJ status, is likely to be required.

Abstract

Purpose: DNA damage defects are common in ovarian cancer and can be used to stratify treatment. Although most work has focussed on Homologous Recombination (HR), DNA double strand breaks are repaired primarily by non-homologous end joining (NHEJ). Defects in NHEJ have been shown to contribute to genomic instability and have been associated with the development of chemoresistance.

Experimental Design: NHEJ was assessed in a panel of ovarian cancer cell lines and 47 primary ascitic derived ovarian cancer cultures, by measuring the ability of cell extracts to end-join linearized plasmid monomers into multimers. mRNA and protein expression of components of NHEJ was determined using RT-qPCR and western blotting. Cytotoxicities of cisplatin and the Poly(ADP-ribose) polymerase-1 (PARP) inhibitor rucaparib were assessed using sulforhodamine B (SRB) assays. HR function was assessed using γH2AX/RAD51 foci assay.

Results: NHEJ was defective (D) in 4 of 6 cell lines and 20 of 47 primary cultures. NHEJ function was independent of homologous recombination (HR) competence (C). NHEJD cultures were resistant to rucaparib ($p=0.0022$). When HR and NHEJ functions were taken into account, only NHEJC/HRD cultures were sensitive to rucaparib (compared to NHEJC/HRC $p=0.034$, NHEJD/HRC $p=0.0002$, and NHEJD/HRD $p=0.0045$). The DNA-PK inhibitor, NU7441 induced resistance to rucaparib ($p=0.014$) and HR function recovery in a BRCA1 defective cell line.

Conclusion: This study has shown that NHEJ is defective in 40% of ovarian cancers, which is independent of HR function and associated with resistance to PARP inhibitors in *ex vivo* primary cultures.

Introduction

Double strand breaks (DSBs) [1], the most lethal forms of DNA damage, are repaired by two main pathways: non-homologous end-joining (NHEJ) and homologous recombination (HR). These pathways are distinct in that HR copies identical DNA sequences from sister chromatids resulting in error-free repair [2], whilst NHEJ joins the broken DNA ends with limited processing [3]. *In vitro* studies have demonstrated that complementary DNA ends are joined in an efficient and accurate manner by NHEJ [4, 5]. However, the modification required for partially or completely incompatible DNA ends results in losses of sequence at the resultant junctions, such that NHEJ is potentially a mutagenic process [3, 6]. More recent studies have demonstrated an alternative end joining mechanism (A-EJ), which uses regions of microhomology at internal sites on the DNA substrate. Unlike HR, A-EJ is inherently error-prone as the use of microhomology leads to deletions of sequences from the strand being repaired, and to chromosomal translocations [7, 8]. This mechanism has been suggested to function in the absence of NHEJ [9-14] and more recently in absence of HR [7, 8].

NHEJ has been demonstrated to function throughout the cell cycle [1, 15]. The NHEJ pathway is initiated by the binding of the Ku heterodimer (Ku70 and Ku80) to DSBs, and the subsequent association and autophosphorylation of the DNA-dependent protein kinase catalytic subunit (DNA-PK_{cs}) [16]. This DNA-PK complex facilitates ligation by recruitment of the XRCC4/LIG4 complex. Mutations in NHEJ components are associated with immunodeficiency and developmental abnormalities [17, 18] as well as cancers [6, 19-22], underscoring the importance of the NHEJ pathway in maintaining genome integrity.

DNA damage repair is increasingly recognized as an important determinant of response to cancer therapeutics. This interest was initially provoked by the paradigm shifting discovery that inhibition of base excision repair with Poly(ADP-ribose) polymerase-1 (PARP-1) inhibitors (PARPi) was synthetically lethal in HR defective (HRD) tumours. PARPi were therefore selectively targeting the defect arising in the tumour, but not in normal tissues [23-27]. In epithelial ovarian cancer (EOC) HRD is reported in 50% of cases [28] and evidence is building for the efficacy of PARPi. This has been assumed to be as a result of synthetic lethality, with PARPi preventing effective base excision repair leading to stalled replication forks which in turn could not be repaired by homologous recombination. However a number of studies also indicate a connection between components of the NHEJ pathway and PARP-1

[29-35], culminating in the suggestion by Patel et al that dysfunctional NHEJ is important in generating genomic instability in PARPi treated, homologous recombination defective, cells [36]. Moreover, they also demonstrated that inhibition of DNA-PK results in HR function recovery and PARPi resistance *in vitro* [37].
The suggestion that NHEJ status is important in determining sensitivity to PARP inhibitors is in keeping with evidence that NHEJ is a fast pathway which is the pathway of choice for the repair of DSBs with HR only being employed for unrepaired DSBs [38].

The incidence of NHEJ dysfunction has not been explored in primary EOC to date. Here we demonstrate that more than 40% of primary ovarian cancer (PCO) cultures are NHEJ defective (NHEJD), which is associated with resistance to rucaparib *ex vivo*.

Materials and Methods

Cell culture

Ethical approval was granted (12/NW/0202) for the collection of ascites from consented patients undergoing surgery for EOC at the Queen Elizabeth Hospital, Gateshead, UK. Clinical details were recorded and specimens registered and handled in accordance with the Human Tissue Act. Samples were assigned a reference number to retain anonymity.

PCO cultures were generated and maintained as previously described [39, 40]. Briefly 20ml of ascites was added to 20ml of warmed Sigma RPMI 1460 HEPES modified culture medium supplemented with 20% v/v fetal calf serum and 100µl/ml penicillin and streptomycin in T75 flasks and incubated at 37°C, 5% CO_2 humidified air.

Cell lines

All cell lines, unless stated otherwise, were grown in RPMI 1640 media supplemented with 10% FBS and 100 units/ml penicillin/streptomycin incubated at 37°C in 5% CO_2. V3 (DNA-PK_{CS} defective) and V3YAC cells (V3 cells complemented with human DNA-PK_{CS}) were a kind gift from Professor Jeggo. V3YAC cells were grown in full medium with G418 (400 µg/ml). A2780, a human ovarian carcinoma cell line and CP70, MMR deficient variant of A2780, 5-fold resistant to cisplatin relative to the parental A2780 were a kind gift from Prof. R. Brown (Cancer Research UK Beatson Laboratories, Glasgow, Scotland). SKOV-3, OVCAR-3, IGROV-1, and MDAH are all human ovarian adenocarcinoma cell lines and were purchased from American Type Culture Collection (ATCC, VA, USA). PEO1 cell line was

derived from a poorly differentiated serous adenocarcinoma and PEO4 cell line derived from the same patient after clinical resistance developed to chemotherapy. Both were purchased from the European Collection of Cell Cultures.

OSEC2 and OSEC4 cell lines developed at Newcastle University from normal ovarian surface epithelium using a temperature sensitive SV-40 large T antigen construct were incubated at 33^{o}C [41].

UWB1-289 is a BRCA1-null human EOC cell line derived from papillary serous ovarian carcinoma was cultured in 50% RPMI 1640 media supplemented with 10% FBS and 100 units/ml penicillin/streptomycin and 50% (v/v) MEBM BulletKit media (Lonza) supplemented with 10% FBS. UWB1-289-BRCA1 is derived from UWB1-289 cells in which BRCA1 was restored were cultured in full media with 400 μg/ml G418. Both were obtained from American Type Culture Collection.

Cell-free extract preparation

Cell extracts were prepared as previously described [6]. Briefly, three T175 flasks at 80% confluence were trypsinised, lysed in 500μl of hypotonic buffer and homogenized. After the addition of 0.5 vol of high salt buffer, the extracts were centrifuged for 56 min at 70,000RPM (213,000g) at 4°C in a Beckman TLA120.2 rotor. Protein concentration was determined using the BSA protein assay according to manufacturer's instructions (ThermoScientific). Samples were snap-frozen and stored at −80°C.

DNA end-joining assay

Vectors which on digestion with BstXI yielded a 3.2 kb plasmid and 1.2 kb λ fragment with either compatible (Co) (CCACTAAG_GTGG and GGTG_ATTCCACC) or 2 base pair (2I) (CCACTAAG_GTGG and GGTG_AAACCACC) and 4 base pair (4I) (CCACTAAG_GTGG and GGTG_TAAGCACC) incompatible ends. Vectors were kindly donated by Dr Ann Kiltie (Oxford, UK). DNA fragments were gel-purified using spin columns (Qiagen, UK). End-joining reactions were carried out as previously described [6] with 45 μg protein extract and 100ng DNA substrate for 2.5 hours. DNA was extracted with Tris-buffered phenol/chloroform/isoamyl alcohol. Analysis was performed by agarose (0.7%) gel electrophoresis and GelRed (VWR) staining. Image capture was carried out using G:Box and GeneSnap system, and analysed using GeneTools (SynGene).

PCR amplification of rejoined products

For the analysis of joined products, end-joining reactions were ethanol-precipitated and amplified using ThermoPrimeTaq with ReadyMix PCR buffer (Thermo Scientific, UK) in the presence of internal plasmid primers pFOR (5′-CCGGCGAACGTGGCGAGAAAG) and pREV (5′-GACTGGAAAGCGGGCAGTGAG) for 40 cycles (30s at 94°C, 30s at 55°C, 30s at 72°C, full length product size 551 bp). Analysis was performed by agarose (1%) gel electrophoresis and GelRed staining.

Intracellular end joining assay

Plasmid pGL2 (Promega) was linearized using either *Hind*III or *Eco*RI, linearization was confirmed by agarose gel electrophoresis. The linearized DNA was purified using the QIAquick PCR Purification Kit, (Qiagen), dissolved in sterilized water, and transfected into cells using Lipofectamine LTX (Invitrogen) as per manufacturer's instructions. The transfectants were harvested 48 hours after transfection and assayed for luciferase activity as described previously [42].

Homologous recombination assay

Cells were seeded onto glass cover slips and treated with 2 Gy ionising radiation and rucaparib at 10 μM concentration for 24 hours to induce double strand breaks (DSB). All experiments were performed alongside untreated controls with equivalent 0.1% DMSO. Cells were then fixed and rehydrated prior to staining with 1:100 mouse monoclonal anti-γH2AX (Upstate, Millipore Corp., USA) and 1:100 goat polyclonal anti-Rad51 (Calbiochem, EMD Biosciences, Inc., USA) antibodies with appropriate secondary fluorochrome conjugated antibodies, as previously described [43].

Image J counting software [44, 45] was used to count γH2AX and Rad51 nucleic foci. Cells were classed as homologous recombination (HR) competent if there was more than a 2 fold increase in Rad51 foci after DNA damage, confirmed by a 2 fold increase in γH2AX.

Reverse transcription and real time PCR

Extraction of RNA was performed using an RNeasy Mini kit (Qiagen) as per manufacturer's instructions. RNA was eluted in 30μl RNase-free water and quantified on the Nanodrop ND-1000 Spectrophotometer (Lab tech International). 1.6μg of the total RNA was incubated at 65˚C for 5 min followed by 37˚C for 5 min prior to addition of Promega MMLV-reverse

transcriptase master mix (4µl 5x Moloney Murine Leukaemia Virus RT buffer, 2µl 4mM dNTPs, 1µl 50µM Oligo dT15and 0.3µl MMLV reverse transcriptase) and incubation at 37˚C for 1 hour followed by 95˚C for 5 min. 2µl of cDNA was loaded on to a 386 well plate in triplicate with Invitrogen SYBR green Master Mix (dNTPs, optimised buffer, UDG, ROX reference dye, AmpliTaq DNA polymerase UP and SYBR green ER dye) and the 2.5mM of the appropriate forward and reverse primers. Primers used were purchased from Sigma Aldrich, Primers sequences were - DNAPK-1 5'–CTAACTCGCCAGTTTATCAATC–3'; 5'–TTTTTCCAATCAAAGGAGGG–3'; DNA-PK-2 5'–GATCTGAAGAGATATGCTGTG–3'; 5'–GTTTCAGAAAGGATTCCAGG–3'; XRCC5 5'-TTCATTCAGTGAGAGTCTGAG-3'; 5'-CGATTTATAGGCTGCAATCC-3'; XRCC6 5'-AAGAAGAGTTGGATGACCAG-3'; 5'-GTCACTTCTGTATGTGAAGC-3'; LIG4 5'-ATTTCTCCCGTTTTTGACTC-3'; 5'-GAATCTTCTCGTTTAACTGGC-3'; XRCC4-1 5'-AGCTGCTGTAAGTAAAGATG-3'; 5'-CCAAGATTTCTTTGCATTCG-3'; XRCC4-2 5'-CCAAGTAGAAAAAGGAGACAG-3'; 5'-GCTTTTCCTTTTCTTGAAGC-3'; XRCC4-3 5'-CTAGAGAAAGTTGAAAACCCAG-3'; 5'-ATCGTCCTTGAACATCATTC–3'; GAPDH 5'–CGACCACTTTGTCAAGCTCA–3'; 5'–GGGTCTTACTCCTTGGAGGC–3'. Samples were run on an AbiPrism Applied Biosystems real time PCR machine for 10min at 95˚C, 40 cycles (15s at 95˚C, 60s at 60˚C), 15s at 95˚C, 15s at 60˚C, 15s at 95˚C. Data was analysed using SDS2.3 software.

Gel electrophoresis and western blotting

Western blotting was assessed as previously described [46]. Briefly, 40µg of total protein from each samples was loaded and resolved by electrophoresis in 3-8% SDS-PAGE gradient gels (Biorad), and transferred to nitrocellulose membrane (Hybond C Membrane (GE Healthcare). Blots were then incubated using appropriate antibodies: DNA-$PK_{cs,}$ [1:500, at 4^{o}C, overnight (ON) (SantaCruz Biotechnology)]; Ku70 [1:800, at 4^{o}C, ON (abcam, UK)]; Ku80 [1:800, at 4^{o}C, ON (abcam, UK)]; XRCC4 [1:1000, at 4^{o}C, ON (AbDSerotec, UK)]; Ligase IV [1:800, at 4^{o}C, ON (Abcam, UK)]; GAPDH [1:3000, at room temperature (RT), for 1 hr (Santa Cruz)]. Followed by HRP-conjugated, Goat anti-rabbit or Goat anti-mouse IgG-HRP secondary antibody [1:1000 at RT, for 1 hr, (Dako, Cambridge, UK)]. Image capture and analysis was carried out using the Fuji LAS-300 Image Analyser System (FujiFilm).

SRB assay

Sulforhodamine B (SRB) assay was used to assess cytotoxicity and cell growth as previously described [47]. Briefly, cells were seeded at a concentration of 1000 cells/well and after adherence, treated with different concentrations of rucaparib or cisplatin +/- 1μM of DNA-PK inhibitor NU7441 for 10 days before fixation, staining and spectrophotometer assessment.

Immunofluorescence

Immunofluorescence experiments were carried out as previously described [43]. Briefly, cells were fixed after 24 hours with 10 μM rucaparib +/- 1 μM NU7441 and 2 Gy X-ray irradiation for HR assay or 1 hour after 2 Gy irradiation for pDNA-PKcs. The γH2AX, RAD51 or pDNA-PKcs foci were detected by immunofluorescence using appropriate antibodies. Anti-phospho-histone γH2AX (Ser139) [1:100 dilution, at RT, for 1 hr (Upstate, Millipore Corporation, USA)]; Rabbit polyclonal anti-Rad51 [1:100 dilution, at 4^{o}C, ON (Calbiochem, EMD Biosciences, Inc.)]; or DNA-PKcs phospho S2056 [1:500 dilution, at 4^{o}C, ON (Abcam, UK)]. Followed by Alexa Fluor 546 Goat anti-mouse or 488 Goat anti- Rabbit IgG secondary antibody [1:1000 dilution at RT, for 1 hr, protected from light (Invitrogen, USA)]. Images were captured using a Leica DMR microscope and RT SE6 Slider camera Advanced Spot software version 3.408 (Diagnostic Instruments Inc. Sterling Heights, USA). Automated analysis using ImageJ software and a custom macro of foci in > 50 cells per field of view was carried out.

PARP-1 activity

PARP-1 activity was measured using a validated assay as previously described [48]. Briefly, PARP activity in 1000 permeabilised cells was maximally stimulated with a double-stranded oligonucleotide in the presence of excess NAD (350 μM) and the amount of ADP-ribose polymer formed quantified by immunoblot using anti-PAR antibody (clone 10H, from Professor Dr Alex Burkle University of Konstanz) by reference to a PAR standard curve (Enzo Life Sciences, Exeter, UK). Data is expressed as % PAR of L1210 control.

Statistical Analysis

Statistical analysis was performed using GraphPad Prism version 6.00 (GraphPad Software, La Jolla California USA) Unpaired student *t* tests or Mann–Whitney tests were used depending on a D'Agostino & Pearson omnibus normality test. Multiple comparisons were

performed using 1-way Anova with Tukeys multiple comparisons correction. All statistical tests were two-sided and considered statistically significant if the *P* value was less than 0.05.

Results

End-joining accuracy depends on DSB compatibility and NHEJ function

A number of assays are described in the literature to assess NHEJ function [49]. Most of these assays only assess the rejoining of compatible ends, which does not represent the complexity of DNA DSBs that occur in cells. We therefore assessed rejoining of compatible (Co) and incompatible (2I - containing mismatches of two bases, and 4I - containing mismatches of 4 bases) vector ends following the addition of cell extracts. T4ligase ligated Co substrates, but incompatible substrates (2I and 4I) could not be joined without the addition of the appropriate λDNA fragment which formed compatible ends with each 2I and 4I substrates (Figure 1.A). OSEC2 cells rejoined 34.8% of Co, 15.9% of 2I and 13.7% of 4I substrates (Figure 1.A-B). Addition of the λDNA fragment increased the rejoining rate of incompatible ($p<0.001$ of 2I and $p=0.0004$ of 4I), but had no effect on rejoining of the compatible substrates. As both 2I and 4I had similar rejoining rates, assessment in cell lines and PCO panels was performed using Co and 2I substrates only. Comparison of rejoining in paired DNA-PK deficient and proficient cell lines demonstrated that whilst compatible ends are largely rejoined correctly, DNA-PK deficient V3 and M059J cells were unable to rejoin 2I substrates (Figure 1.C). Furthermore addition of DNA-PK inhibitor NU7441 inhibited rejoining in DNA-PKcs proficient V3YAC cells, but had no effect on DNA-PKcs deficient V3 cells (Figure 1.D).

DNA end joining in established EOC cell lines

To ensure the cell free extract assay represented the cellular end joining accurately, NHEJ function was assessed in a panel of established cell lines using the cell extract and a cellular luciferase assay (Figure 2). Whilst the OSEC cell lines derived from normal ovarian epithelium were able to rejoin 2I ends accurately, four of the six EOC cell lines were unable to rejoin 2I substrates, thus indicating NHEJ deficiency. This correlated with the cellular end joining assay. Mean accurate cellular rejoining rate was 30.17%, 95% confidence interval (CI) = 25-37.6% by cell lines able to rejoin 2I substrates compared to 9.9%, 95% CI 4.39-14.0, $p=0.03$ by cell lines unable to rejoin 2I substrates, when assessed using the luciferase cellular assay (Pearson correlation $r = 0.79$ $p=0.007$). We have previously demonstrated that

vector transfection into PCO cultures is not possible [39], therefore NHEJ was assessed in PCO cultures with the validated extract assay only.

PCO cultures rejoin compatible DSBs, but 40% are unable to rejoin mismatched DSBs

We next assessed end joining in a panel of primary ovarian cancer cultures. PCO cultures had a reduced end joining rate compared to NHEJ competent (NHEJC) control cell lines. There was significant inter-sample variability (range 5% to 39% of loaded DNA, Figure 3.A-B). PCR analysis of the junctions formed demonstrated that the rejoining of the Co substrate was accurate (Figure 3.C).

We found that 20 of the 47 PCO cultures were NHEJD, as demonstrated by incubation with 2I substrates producing either no products, or forming products of significantly smaller size (Example PCR product bands is shown in Figure 3.C). Furthermore, some cultures formed multiple bands of different sizes indicating loss of differing numbers of nucleotides. Extensive resection has been demonstrated to be due to use of microhomologies in this vector in the absence of a functional NHEJ pathway [6]. NHEJ competence was seen to be independent of culture growth rate, with a mean doubling time of 117 hours for NHEJC and 115 hours for NHEJD cultures. Patient characteristics detailed in Supplementary Table ST1 show that there was no significant difference between the NHEJC and NHEJD cultures in any of the clinical parameters assessed.

Sensitivity to rucaparib but not cisplatin is dependent upon competent NHEJ function

Sensitivity of rucaparib and cisplatin was assessed in the cell line panel and all primary cultures. In contrast to HRD association with increased rucaparib sensitivity, NHEJD cultures were resistant to rucaparib ($p=0.0022$, figure 4.A), as well as established cell lines ($p<0.0001$) (Figure 4.B). Furthermore, NU7441 induced resistance to rucaparib in the sensitive PCO cultures ($p=0.014$). When HR and NHEJ functions were taken into account, only NHEJC/HRD cultures were sensitive to rucaparib (compared to NHEJC/HRC $p=0.034$, NHEJD/HRC $p=0.0002$, and NHEJD/HRD $p=0.0045$).

No correlation of cisplatin sensitivity was found with NHEJ function or inhibition (Figure 4.C). Cisplatin was found to inhibit NHEJ significantly even at 4nM concentration (Figure 4.D). This was consistent with the finding of no association of NHEJ function with progression free survival (PFS) or overall survival in our cohort of patients who were treated

with a standard platinum based therapy after a median follow up of 20 months Supplementary Table ST1.

Protein expression of Ku70, Ku80 and DNAPK, but not DNA-PK phosphorylation, may serve as a biomarker of NHEJ function

Analysis of NHEJ pathway components showed that protein expression of Ku70, Ku80 and DNA-PKcs, normalised to GAPDH, were all significantly lower in NHEJD cultures (Ku70 $p=0.0013$, Ku80 $p=0.002$ and DNA-PKcs $p<0.0001$, figure 5.A). These were found to be good predictors (AUC 0.798, 0.762 and 0.852 respectively, figure 5.B) for NHEJ function and may therefore be suitable candidates for biomarkers. Discordance between protein and mRNA expression was noted, as previously reported in other studies [50, 51]. DNA-PK autophosphorylation correlated with NHEJ function in cell lines, but not in the PCO cultures (Supplementary figure S1).

Interaction of HR and NHEJ pathways

We have previously demonstrated that 50% of ovarian cultures are functionally HRD [28], therefore upon the finding that 40% of primary ovarian cancer cultures are also NHEJD we assessed the interaction of NHEJ and HR. The addition of the DNA-PK inhibitor, NU7441, resulted in a significant up-regulation of RAD51 foci after 2Gy irradiation in OSEC2 cells (Figure 6.A), demonstrating an increase in HR repair. NU7441 also recovered HR competence in the BRCA1 deficient cell line, but it had no effect in the HR competent or BRCA2 defective cell lines (Figure 6.B). Furthermore, the mean fold rise in RAD51 foci in DNA-PK deficient M059J cells was significantly higher compared to isogenic DNA-PK proficient M059FUS-1 cells ($p < 0.0001$, Figure 7.C).

In our cohort of PCO cultures, NHEJ function was independent of HR competence. 15 cultures were functional for both pathways, 7 cultures were defective for both pathways, while 11 and 14 cultures showed defects in NHEJ and HR respectively. RAD51 foci rise was higher in NHEJD compared to NHEJC cultures ($p<0.0024$, figure 7.A). DNA-PKcs expression was higher in HRC cultures compared to HRD cultures ($p<0.0001$, figure 7.A).). When taking both HR and NHEJ function into account, whilst both NHEJC/HRC and NHEJD/HRC were found to have RAD51 foci fold rise >2, the mean RAD51 foci fold rise for NHEJC/HRC group was lower compared to NHEJD/HRC group (Figure 7.B). The differences in RAD51 foci rise between all four groups was independent of the amount of

DNA DSBs, as determined by γH2AX foci formation. Importantly , no correlation between either PARP-1 activity or mRNA expression and HR or NHEJ competence was found (Supplementary figure 1.C).

Discussion

Here we have described our findings that NHEJ is defective in more than 40% of *ex vivo* EOCs. We found NHEJ to be independent of HR function and PARP-1 activity. In contrast to HR (where cells with the HRD phenotype are sensitive to PARPi) we have demonstrated that cells defective in NHEJ are resistant to PARPi. By considering the function of both pathways, we have shown that only the NHEJC/HRD cultures are sensitive to rucaparib. This finding potentially explains the resistance observed in some HRD tumours. Finally, we suggest that expression of the NHEJ related proteins Ku70, Ku80 and DNA-PKcs may be useful as biomarkers to determine NHEJ status in cancer samples.

The sensitivity of HRD cancers to PARPi was initially attributed to the concept of synthetic lethality, based on the theory that HR defective cells are unable to repair DNA DSBs [25, 52]. However, the majority of DNA DSBs are repaired by NHEJ [1, 15]. Furthermore, cell line studies demonstrate interaction between the NHEJ pathway, PARP-1 and subsequent resistance to PARPi [37]. The suggested role for NHEJ in PARPi sensitivity was through up regulation of error prone NHEJ in HRD cells [37]. Recent studies have demonstrated that the error prone A-EJ, functions in the absence of NHEJ and competes with HR [7, 8, 53]. Clearly the interaction between the various DSB repair pathways is complex and understanding is compounded by the commonality of the early part of the process. In this study we weren't able to assess the cell cycle specific of both pathways but this may provide further insight into the interaction [54].

Nevertheless,we have found that NHEJ function is independent of HR competence and that inhibition of NHEJ resulted in up regulation of HR function in HRC and BRCA1 deficient cells. In our cohort, the cultures which were NHEJD were resistant to rucaparib, irrespective of HR function. This is supported by the observation that NU7441 caused rucaparib resistance in all sensitive cultures, independent of HR function. When taking both pathways into account only NHEJC/HRD cultures were found to be sensitive to rucaparib. Here we demonstrate the role of NHEJ function in *ex vivo* primary cultures. Therefore, we propose that in EOC, in the absence of HR, error prone NHEJ results in sensitivity to PARPi. Conversely absence of NHEJ function results in PARPi resistance in HRD cells. This may be

through A-EJ, however assessment of this pathway in primary EOC is still needed. Due to the inhibitory effect of cisplatin on NHEJ [55], this model is limited to rucaparib sensitivity only.

The hypothesis put forward for the role of NHEJ in PARPi resistance is based on the error proneness of NHEJ. The errors in repair are suggested to cause lethal defects in DNA, which, in the absence of HR, results in apoptosis. Therefore, NHEJC/HRD cells are sensitive to PARPi. Cells with competent NHEJ and HR pathways are able to repair DNA damage and are, therefore, resistant to PARPi. In the absence of NHEJ, the slower error free HR takes over repair. This notion is supported by findings of greater HR function, demonstrated by greater RAD51 foci formation in the DNA-PK deficient cell lines in this study as well as the existing literature [56]. Therefore, in the absence of NHEJ function, the lack of error prone repair results in resistance to PARPi [37].

Our finding of selectivity for a DNA-PKcs inhibitor to selectively revert the BRCA1 mutant cell line but not the BRCA2 mutant line is interesting but can be explained by the differing functions of BRCA1 and BRCA2 in the DDR pathways. The role of BRCA1 is to inhibit Rif1 which in turn selects for NHEJ. HR can still therefore function in the absence of BRCA1 but preferentially cells will proceed down the NHEJ pathway because there is no inhibition of Rif1 and therefore no inhibition of NHEJ. But if NHEJ is inhibited or defective, even without BRCA1, HR can go ahead.

The role of BRCA2 is within HR pathway itself. Therefore inhibiting NHEJ in the absence of BRCA2 still does not activate HR because HR itself is broken.

The ability to select the correct patient, for the correct treatment, at the right time, is required for personalised medicine. Our findings suggest that accurate selection will be compromised if HR function alone is assessed and assessment of NHEJ may also be required. Whilst attempts are being made to develop predictive biomarkers of HR, we suggest that biomarkers for NHEJ should also be developed in order to aid patient selection for PARPi therapy.

Acknowledgements

We thank Dr Anne Kiltie for the kind donation of vector constructs and the protocol for the end joining assay which allowed this project to take place. We also thank the patients and the clinical staff at Queen Elizabeth Hospital for the PCO sample donation.

References

1. Valerie, K. and L.F. Povirk, *Regulation and mechanisms of mammalian double-strand break repair.* Oncogene, 2003. **22**(37): p. 5792-5812.
2. Helleday, T., *Homologous recombination in cancer development, treatment and development of drug resistance.* Carcinogenesis, 2010. **31**(6): p. 955-60.
3. Lieber, M.R., Y. Ma, U. Pannicke, and K. Schwarz, *Mechanism and regulation of human non-homologous DNA end-joining.* Nat Rev Mol Cell Biol, 2003. **4**(9): p. 712-20.
4. Baumann, P. and S.C. West, *DNA end-joining catalyzed by human cell-free extracts.* Proc Natl Acad Sci U S A, 1998. **95**(24): p. 14066-70.
5. Labhart, P., *Nonhomologous DNA end joining in cell-free systems.* Eur J Biochem, 1999. **265**(3): p. 849-61.
6. Bentley, J., C.P. Diggle, P. Harnden, M.A. Knowles, and A.E. Kiltie, *DNA double strand break repair in human bladder cancer is error prone and involves microhomology-associated end-joining.* Nucleic Acids Res, 2004. **32**(17): p. 5249-59.
7. Ceccaldi, R., J.C. Liu, R. Amunugama, I. Hajdu, B. Primack, M.I. Petalcorin*, et al.*, *Homologous-recombination-deficient tumours are dependent on Poltheta-mediated repair.* Nature, 2015. **518**(7538): p. 258-62.
8. Mateos-Gomez, P.A., F. Gong, N. Nair, K.M. Miller, E. Lazzerini-Denchi, and A. Sfeir, *Mammalian polymerase theta promotes alternative NHEJ and suppresses recombination.* Nature, 2015. **518**(7538): p. 254-7.
9. Pannunzio, N.R., S. Li, G. Watanabe, and M.R. Lieber, *Non-homologous end joining often uses microhomology: implications for alternative end joining.* DNA Repair (Amst), 2014. **17**: p. 74-80.
10. Rai, R., H. Zheng, H. He, Y. Luo, A. Multani, P.B. Carpenter*, et al.*, *The function of classical and alternative non-homologous end-joining pathways in the fusion of dysfunctional telomeres.* EMBO J, 2010. **29**(15): p. 2598-610.
11. Iliakis, G., H. Wang, A.R. Perrault, W. Boecker, B. Rosidi, F. Windhofer*, et al.*, *Mechanisms of DNA double strand break repair and chromosome aberration formation.* Cytogenet Genome Res, 2004. **104**(1-4): p. 14-20.
12. Wang, H., A.R. Perrault, Y. Takeda, W. Qin, and G. Iliakis, *Biochemical evidence for Ku-independent backup pathways of NHEJ.* Nucleic Acids Res, 2003. **31**(18): p. 5377-88.
13. Yan, C.T., C. Boboila, E.K. Souza, S. Franco, T.R. Hickernell, M. Murphy*, et al.*, *IgH class switching and translocations use a robust non-classical end-joining pathway.* Nature, 2007. **449**(7161): p. 478-82.
14. Corneo, B., R.L. Wendland, L. Deriano, X. Cui, I.A. Klein, S.Y. Wong*, et al.*, *Rag mutations reveal robust alternative end joining.* Nature, 2007. **449**(7161): p. 483-6.
15. Curtin, N.J., *DNA repair dysregulation from cancer driver to therapeutic target.* Nat Rev Cancer, 2012. **12**(12): p. 801-17.
16. Walker, J.R., R.A. Corpina, and J. Goldberg, *Structure of the Ku heterodimer bound to DNA and its implications for double-strand break repair.* Nature, 2001. **412**(6847): p. 607-14.
17. O'Driscoll, M., A.R. Gennery, J. Seidel, P. Concannon, and P.A. Jeggo, *An overview of three new disorders associated with genetic instability: LIG4 syndrome, RS-SCID and ATR-Seckel syndrome.* DNA Repair (Amst), 2004. **3**(8-9): p. 1227-35.
18. Sekiguchi, J.M. and D.O. Ferguson, *DNA double-strand break repair: a relentless hunt uncovers new prey.* Cell, 2006. **124**(2): p. 260-2.
19. Bentley, J., C. L'Hote, F. Platt, C.D. Hurst, J. Lowery, C. Taylor*, et al.*, *Papillary and muscle invasive bladder tumors with distinct genomic stability profiles have different DNA repair fidelity and KU DNA-binding activities.* Genes Chromosomes Cancer, 2009. **48**(4): p. 310-21.

20. Windhofer, F., S. Krause, C. Hader, W.A. Schulz, and A.R. Florl, *Distinctive differences in DNA double-strand break repair between normal urothelial and urothelial carcinoma cells.* Mutat Res, 2008. **638**(1-2): p. 56-65.
21. Gaymes, T.J., G.J. Mufti, and F.V. Rassool, *Myeloid leukemias have increased activity of the nonhomologous end-joining pathway and concomitant DNA misrepair that is dependent on the Ku70/86 heterodimer.* Cancer Res, 2002. **62**(10): p. 2791-7.
22. Deriano, L., O. Guipaud, H. Merle-Beral, J.L. Binet, M. Ricoul, G. Potocki-Veronese*, et al.*, *Human chronic lymphocytic leukemia B cells can escape DNA damage-induced apoptosis through the nonhomologous end-joining DNA repair pathway.* Blood, 2005. **105**(12): p. 4776-83.
23. Dantzer, F., V. Schreiber, C. Niedergang, C. Trucco, E. Flatter, G. De La Rubia*, et al.*, *Involvement of poly(ADP-ribose) polymerase in base excision repair.* Biochimie, 1999. **81**(1-2): p. 69-75.
24. Gottipati, P., B. Vischioni, N. Schultz, J. Solomons, H.E. Bryant, T. Djureinovic*, et al.*, *Poly(ADP-ribose) polymerase is hyperactivated in homologous recombination-defective cells.* Cancer Res, 2010. **70**(13): p. 5389-98.
25. Ashworth, A., *A synthetic lethal therapeutic approach: poly(ADP) ribose polymerase inhibitors for the treatment of cancers deficient in DNA double-strand break repair.* J Clin Oncol, 2008. **26**(22): p. 3785-90.
26. Bryant, H.E., N. Schultz, H.D. Thomas, K.M. Parker, D. Flower, E. Lopez*, et al.*, *Specific killing of BRCA2-deficient tumours with inhibitors of poly(ADP-ribose) polymerase.* Nature, 2005. **434**(7035): p. 913-7.
27. McCabe, N., N.C. Turner, C.J. Lord, K. Kluzek, A. Bialkowska, S. Swift*, et al.*, *Deficiency in the repair of DNA damage by homologous recombination and sensitivity to poly(ADP-ribose) polymerase inhibition.* Cancer Res, 2006. **66**(16): p. 8109-15.
28. Mukhopadhyay, A., A. Elattar, A. Cerbinskaite, S.J. Wilkinson, Y. Drew, S. Kyle*, et al.*, *Development of a functional assay for homologous recombination status in primary cultures of epithelial ovarian tumor and correlation with sensitivity to poly(ADP-ribose) polymerase inhibitors.* Clin Cancer Res. **16**(8): p. 2344-51.
29. Pleschke, J.M., H.E. Kleczkowska, M. Strohm, and F.R. Althaus, *Poly(ADP-ribose) binds to specific domains in DNA damage checkpoint proteins.* J Biol Chem, 2000. **275**(52): p. 40974-80.
30. Li, B., S. Navarro, N. Kasahara, and L. Comai, *Identification and biochemical characterization of a Werner's syndrome protein complex with Ku70/80 and poly(ADP-ribose) polymerase-1.* J Biol Chem, 2004. **279**(14): p. 13659-67.
31. Gagne, J.P., M. Isabelle, K.S. Lo, S. Bourassa, M.J. Hendzel, V.L. Dawson*, et al.*, *Proteome-wide identification of poly(ADP-ribose) binding proteins and poly(ADP-ribose)-associated protein complexes.* Nucleic Acids Res, 2008. **36**(22): p. 6959-76.
32. Galande, S. and T. Kohwi-Shigematsu, *Poly(ADP-ribose) polymerase and Ku autoantigen form a complex and synergistically bind to matrix attachment sequences.* J Biol Chem, 1999. **274**(29): p. 20521-8.
33. Wang, M., W. Wu, W. Wu, B. Rosidi, L. Zhang, H. Wang*, et al.*, *PARP-1 and Ku compete for repair of DNA double strand breaks by distinct NHEJ pathways.* Nucleic Acids Res, 2006. **34**(21): p. 6170-82.
34. Couto, C.A., H.Y. Wang, J.C. Green, R. Kiely, R. Siddaway, C. Borer*, et al.*, *PARP regulates nonhomologous end joining through retention of Ku at double-strand breaks.* J Cell Biol, 2011. **194**(3): p. 367-75.
35. Hochegger, H., D. Dejsuphong, T. Fukushima, C. Morrison, E. Sonoda, V. Schreiber*, et al.*, *Parp-1 protects homologous recombination from interference by Ku and Ligase IV in vertebrate cells.* EMBO J, 2006. **25**(6): p. 1305-14.

36. Patel, A.G., J.N. Sarkaria, and S.H. Kaufmann, *Nonhomologous end joining drives poly(ADP-ribose) polymerase (PARP) inhibitor lethality in homologous recombination-deficient cells.* Proceedings of the National Academy of Sciences, 2011. **108**(8): p. 3406-3411.
37. Patel, A.G., J.N. Sarkaria, and S.H. Kaufmann, *Nonhomologous end joining drives poly(ADP-ribose) polymerase (PARP) inhibitor lethality in homologous recombination-deficient cells.* Proc Natl Acad Sci U S A, 2011. **108**(8): p. 3406-11.
38. Shibata, A., S. Conrad, J. Birraux, V. Geuting, O. Barton, A. Ismail*, et al.*, *Factors determining DNA double-strand break repair pathway choice in G2 phase.* The EMBO Journal, 2011. **30**(6): p. 1079-1092.
39. RL, O.D., A. McCormick, A. Mukhopadhyay, L.C. Woodhouse, M. Moat, A. Grundy*, et al.*, *The use of ovarian cancer cells from patients undergoing surgery to generate primary cultures capable of undergoing functional analysis.* PLoS One, 2014. **9**(6): p. e90604.
40. Maloney, K.E., R.W. Norman, C.L. Lee, O.H. Millard, and J.P. Welch, *Cytogenetic abnormalities associated with renal cell carcinoma.* J Urol, 1991. **146**(3): p. 692-6.
41. Davies, B.R., I.A. Steele, R.J. Edmondson, S.A. Zwolinski, G. Saretzki, T. von Zglinicki*, et al.*, *Immortalisation of human ovarian surface epithelium with telomerase and temperature-senstitive SV40 large T antigen.* Experimental Cell Research, 2003. **288**(2): p. 390-402.
42. Bau, D.T., Y.P. Fu, S.T. Chen, T.C. Cheng, J.C. Yu, P.E. Wu*, et al.*, *Breast cancer risk and the DNA double-strand break end-joining capacity of nonhomologous end-joining genes are affected by BRCA1.* Cancer Res, 2004. **64**(14): p. 5013-9.
43. Mukhopadhyay, A., A. Elattar, A. Cerbinskaite, S.J. Wilkinson, Y. Drew, S. Kyle*, et al.*, *Development of a functional assay for homologous recombination status in primary cultures of epithelial ovarian tumor and correlation with sensitivity to poly(ADP-ribose) polymerase inhibitors.* Clin Cancer Res, 2010. **16**(8): p. 2344-51.
44. Abramoff, M., Magelhaes, P., Ram, S., *Image processing with ImageJ.* Biophoton Int, 2004. **11**: p. 36-42.
45. Znojek, P., *PhD Thesis.* Newcastle University, 2011.
46. Abdel-Fatah, T.M., F.K. Middleton, A. Arora, D. Agarwal, T. Chen, P.M. Moseley*, et al.*, *Untangling the ATR-CHEK1 network for prognostication, prediction and therapeutic target validation in breast cancer.* Mol Oncol, 2015. **9**(3): p. 569-585.
47. Vichai, V. and K. Kirtikara, *Sulforhodamine B colorimetric assay for cytotoxicity screening.* Nat Protoc, 2006. **1**(3): p. 1112-6.
48. Plummer, E.R., M.R. Middleton, C. Jones, A. Olsen, I. Hickson, P. McHugh*, et al.*, *Temozolomide pharmacodynamics in patients with metastatic melanoma: dna damage and activity of repair enzymes O6-alkylguanine alkyltransferase and poly(ADP-ribose) polymerase-1.* Clin Cancer Res, 2005. **11**(9): p. 3402-9.
49. Pastwa, E., R.I. Somiari, M. Malinowski, S.B. Somiari, and T.A. Winters, *In vitro non-homologous DNA end joining assays--the 20th anniversary.* Int J Biochem Cell Biol, 2009. **41**(6): p. 1254-60.
50. Guo, Y.F., P. Xiao, S.F. Lei, F.Y. Deng, G.G. Xiao, Y.Z. Liu*, et al.*, *How is mRNA expression predictive for protein expression? A correlation study on human circulating monocytes.* Acta Biochimica Et Biophysica Sinica, 2008. **40**(5): p. 426-436.
51. Chen, G., T.G. Gharib, C.C. Huang, J.M. Taylor, D.E. Misek, S.L. Kardia*, et al.*, *Discordant protein and mRNA expression in lung adenocarcinomas.* Mol Cell Proteomics, 2002. **1**(4): p. 304-13.
52. Helleday, T., H.E. Bryant, and N. Schultz, *Poly(ADP-ribose) polymerase (PARP-1) in homologous recombination and as a target for cancer therapy.* Cell Cycle, 2005. **4**(9): p. 1176-8.
53. Nik-Zainal, S., L.B. Alexandrov, D.C. Wedge, P. Van Loo, C.D. Greenman, K. Raine*, et al.*, *Mutational processes molding the genomes of 21 breast cancers.* Cell, 2012. **149**(5): p. 979-93.

54. Mjelle, R., S.A. Hegre, P.A. Aas, G. Slupphaug, F. DrablV∏s, P.l. Sv¶trom*, et al.*, *Cell cycle regulation of human DNA repair and chromatin remodeling genes.* DNA Repair, 2015. **30**: p. 53-67.
55. Diggle, C.P., J. Bentley, M.A. Knowles, and A.E. Kiltie, *Inhibition of double-strand break non-homologous end-joining by cisplatin adducts in human cell extracts.* Nucleic Acids Res, 2005. **33**(8): p. 2531-9.
56. Middleton, F.K., M.J. Patterson, C.J. Elstob, S. Fordham, A. Herriott, M.A. Wade*, et al.*, *Common cancer-associated imbalances in the DNA damage response confer sensitivity to single agent ATR inhibition.* Oncotarget, 2015. **6**(32): p. 32396-409.

Figure legends

Figure 1. Rejoining of BstXI compatible (Co), 2 base mismatch (2I) and 4 base mismatch (4I) substrates. **A.** Rejoining of BstXI compatible (Co), 2 base mismatch (2I) and 4 base mismatch (4I) substrates with or without addition of λ substrate by T4ligase and OSEC2 cell line. Agarose gels are representative of 3 independent experiments. Successful rejoining is demonstrated by the presence of multimer bands. **B.** Densitometry quantification of OSEC2 rejoining results are expressed as total rejoined products / total DNA loaded. Error bars are SEM. **C.** PCR analysis of rejoined DNA of BstXI Co or 2I substrates by V3YAC (DNA-PKcs corrected), V3 (DNA-PKcs deficient), M059FUS-1 (DNA-PKcs corrected) andM059J (DNA-PKcs deficient) cell lines amplified using pFOR and pREV primers. Correct rejoining produces products of 551bps. Inaccurate rejoining with loss of bases results in smaller or no product formation. Gels are representative of 3 independent experiments. **D.** Rejoining of Co substrates by V3YAC and V3 cell lines with addition of increasing concentration of NU7741. Rejoining is demonstrated by formation of multimer bands. Gels are representative of three independent experiments.

Figure 2. End joining by immortalised cell lines. **A.** End joining of compatible BstXI substrates by ovarian cell lines. Gels are representative of 3 independent experiments **B.** End joining of 2I BstXI substrates by ovarian cell lines. Gels are representative of 3 independent experiments. **C.** Intracellular end joining of linearised pGL2 vector by ovarian cell lines measured by luciferase expression. Measured as precise rejoining / overall end joining x 100. Data are average of three independent experiments. Error bars are SEM. **D.** Correlation of rejoining by the two assays.

Figure 3. End joining of BstXI substrates by PCO cultures. **A.** Quantification of PCO rejoining of Co substrates. Results are representative of 3 independent experiments. OSEC2 and V3YAC (DNA-PKcs corrected) were used as positive controls. V3 (DNA-PKcs deficient) cell line was used as a negative control. Water was used as a contamination control. Error bars are SEM. PCO N = 47. **B.** Representative image of GelRed detection of end joining of BstXI compatible substrates by PCO cultures. **C.** Representative image of PCR analysis of rejoined DNA of Co and 2I substrates amplified using pFOR and pREV primers. Correct rejoining produces products of 551bps. Inaccurate rejoining with loss of bases results in smaller or no product formation.

Figure 4. Rucaparib and cisplatin cytotoxicity in PCO cultures and cell lines. **A.** Cell survival calculated as cell growth after 10 days treatment with 10μM rucaparib as a fraction of DMSO control growth for PCO cultures was assessed by SRB assay and results were divided by NHEJ and HR status. Error bars are SEM. N = 47. In addition to treatment with rucaparib cells were also treated with 1μM NU7441 and normalised to DMSO controls. Results for cultures sensitive to rucaparib (< median survival) are presented. N = 22. **B.** Cell survival after 10 days treatment with 10μM rucaparib or 10μM cisplatin for immortalised cell lines assessed by SRB assay and results were divided by NHEJ status. Error bars are SEM. N = 8. **C.** Cell survival calculated as cell growth after 10 days treatment with 10μM cisplatin as a fraction of H_2O control growth for PCO cultures was assessed by SRB assay and results were divided by NHEJ and HR status. Error bars are SEM. N = 42. In addition to treatment with cisplatin cells were also treated with 1μM NU7441 and normalised to DMSO control. N = 42. **D.** Cisplatin inhibition of end joining of compatible and incompatible BstXI digested substrates by OSEC2 cell line. Results are average of three independent experiments. Error bars are SEM.

Figure 5. Prediction of NHEJ function by mRNA and protein expression of pathway components **A.** mRNA and protein expression of NHEJ components PCO cultures assessed by RT-qPCR and western blotting. Western bands were quantified using Fuji LAS-300 Image Analyser System. Protein and mRNA levels were normalised to GAPDH expression. Results are average of 3 independent experiments. Error bars are SEM. N = 47. **B.** ROC curves for Ku70, Ku80 and DNA-PKcs protein expression as predictors of NHEJ function. ROC curves were generated and AUC calculated using PRISM software.

Figure 6. The effect of DNA-PK inhibition on HR function. **A.** HR function after DNA-PK inhibition. RAD51 foci fold rise above un-irradiated controls over time after 2Gy irradiation in OSEC2 cell line +/- 1μM NU7441 treatment. Foci were counted across 3 fields of view for each sample counting >50 cells in each sample. Results are average of 3 independent experiments. **B.** HR competence assessed by a 2 fold increase in RAD51 foci formation above DMSO treated controls after 24 hours of 10 μM rucaparib and 2 Gy IR treatment in BRCA1 and BRCA2 deficient and proficient paired cell lines +/- 1μM NU7441. Cell lines used were UWB1-289 cell line which carries a germline BRCA1 mutation within exon 11 and a deletion of the wild-type allele and paired UWB1.289+BRCA1 cell line in which wild type BRCA1 has been restored. BRCA2 paired cell lines were PEO1 which carries 5193C>G (Y1655X) BRCA2 mutation and PEO4 which was derived from the same patient and carries a secondary BRCA2 mutation [5193C>T (Y1655Y)] that restores BRCA2 function. RAD51 foci were assessed as mean foci count per cell compared to untreated controls. Foci were counted across 3 fields of view for each sample counting >50 cells in each sample. Results are average of 3 independent experiments. Error bars are SEM. **C.** RAD51 and γH2AX focus formation was assessed 24 hrs after 2 Gy irradiation compared to untreated controls. Foci were counted across > 100 nuclei and results are expressed as fold rise above controls.

Figure 7. Interaction of NHEJ and HR pathways in PCO cultures. **A.** RAD51 foci were assessed as mean foci count per cell in samples after 24 hours of 10 μM rucaparib and 2 Gy IR treatment. Foci were counted across 3 fields of view for each sample counting >50 cells in each sample. Results are expressed as fold rise above DMSO treated controls. DNA-PK protein expression was assessed by western blotting and normalised to GAPDH house keeper gene. Error bars are SEM. RAD51 foci and DNA-PK expression results were divided by NHEJ and HR function. **B.** DNA damage was assessed by γH2AX foci rise and HR function by RAD51 foci rise after 24 hours of 10 μM rucaparib and 2Gy IR treatment compared to DMSO treated controls. Results were divided by NHEJ and HR function.

Figure 1

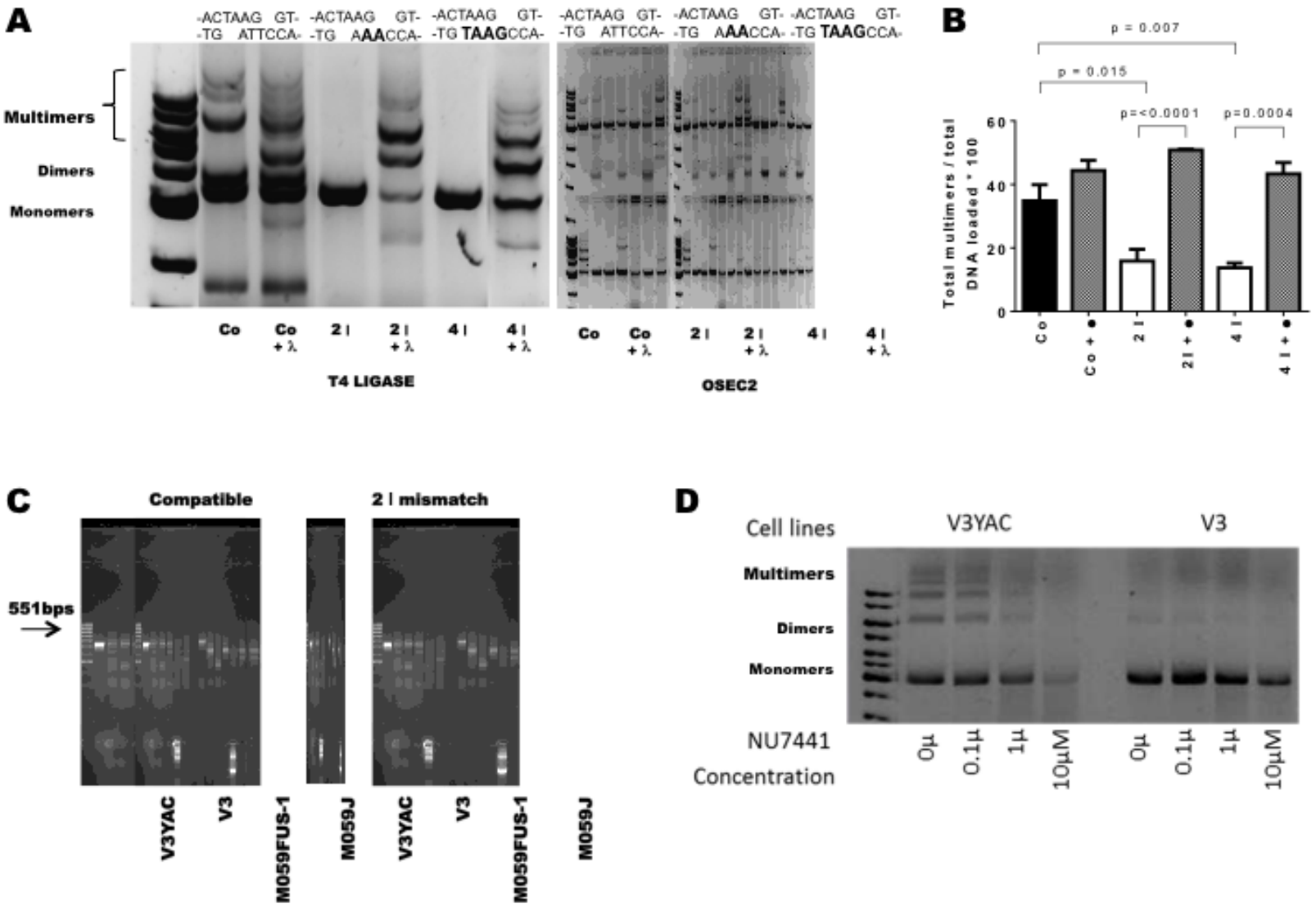
A
-ACTAAG GT-
-TG ATTCCA-
-ACTAAG GT-
-TG AAACCA-
-ACTAAG GT-
-TG TAAGCCA-
Multimers
Dimers
Monomers
Co
Co + λ
2 I
2 I + λ
4 I
4 I + λ
T4 LIGASE
OSEC2
B
p = 0.007
p = 0.015
p=<0.0001
p=0.0004
Total multimers / total DNA loaded * 100
60
40
20
0
Co
Co + ●
2 I
2 I + ●
4 I
4 I + ●
C
Compatible
2 I mismatch
551bps
V3YAC
V3
M059FUS-1
M059J
V3YAC
V3
M059FUS-1
M059J
D
Cell lines
V3YAC
V3
Multimers
Dimers
Monomers
NU7441
Concentration
0µ
0.1µ
1µ
10µM
0µ
0.1µ
1µ
10µM

Figure 2

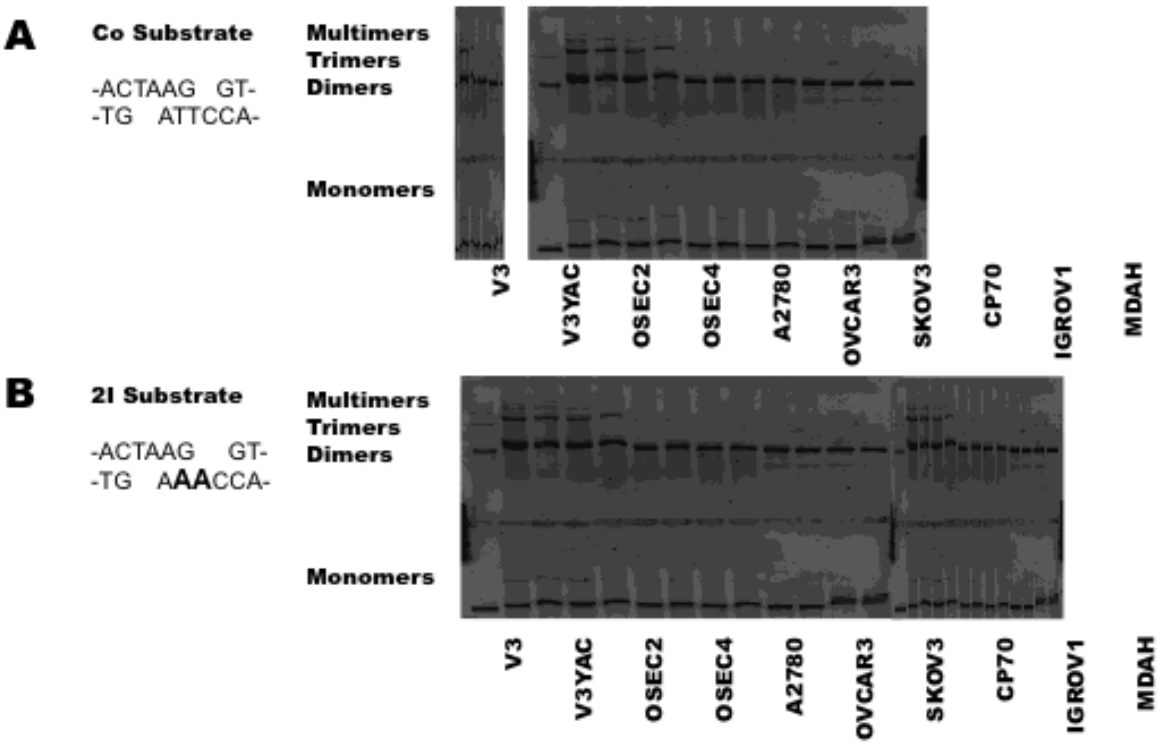
A
Co Substrate
-ACTAAG GT-
-TG ATTCCA-
Multimers
Trimers
Dimers
Monomers
V3
V3YAC
OSEC2
OSEC4
A2780
OVCAR3
SKOV3
CP70
IGROV1
MDAH
B
2I Substrate
-ACTAAG GT-
-TG AAACCA-
Multimers
Trimers
Dimers
Monomers
V3
V3YAC
OSEC2
OSEC4
A2780
OVCAR3
SKOV3
CP70
IGROV1
MDAH

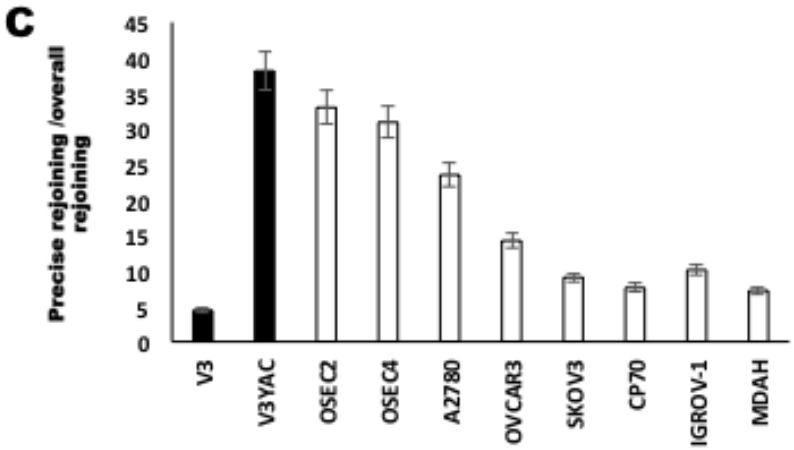
C
Precise rejoining /overall rejoining
45
40
35
30
25
20
15
10
5
0
V3
V3YAC
OSEC2
OSEC4
A2780
OVCAR3
SKOV3
CP70
IGROV-1
MDAH

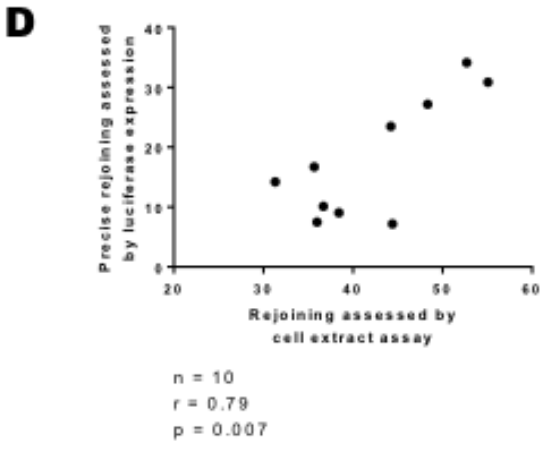
D
Precise rejoining assessed by luciferase expression
40
30
20
10
0
20
30
40
50
60
Rejoining assessed by cell extract assay
n = 10
r = 0.79
p = 0.007

Figure 3

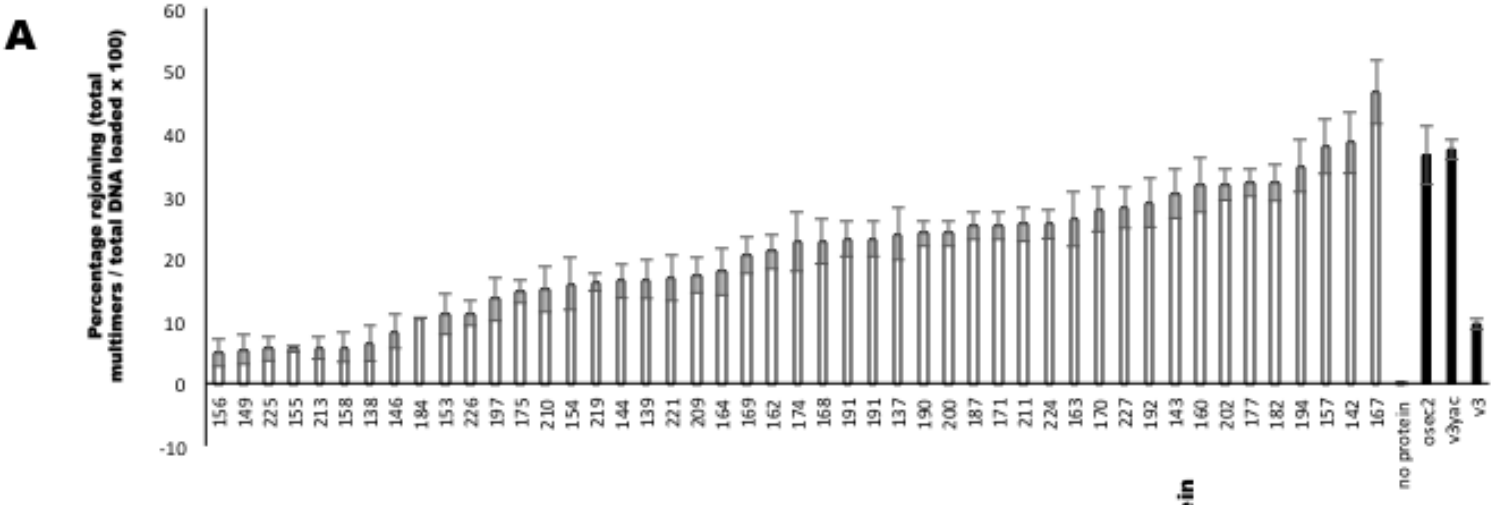
A
Percentage rejoining (total multimers / total DNA loaded x 100)
60
50
40
30
20
10
0
-10
156 149 225 155 213 158 138 146 184 153 226 197 175 210 154 219 144 139 221 209 164 169 162 174 168 191 191 137 190 200 187 171 211 224 163 170 227 192 143 160 202 177 182 194 157 142 167 no protein osec2 v3yac v3
B
184 162 142 156
Multimers
Trimers
Dimers
Monomers
C
162 142 156 184 No protein OSEC2 V3YAC V3
Co Substrate
551bps
2l substrate
551bps

Figure 4

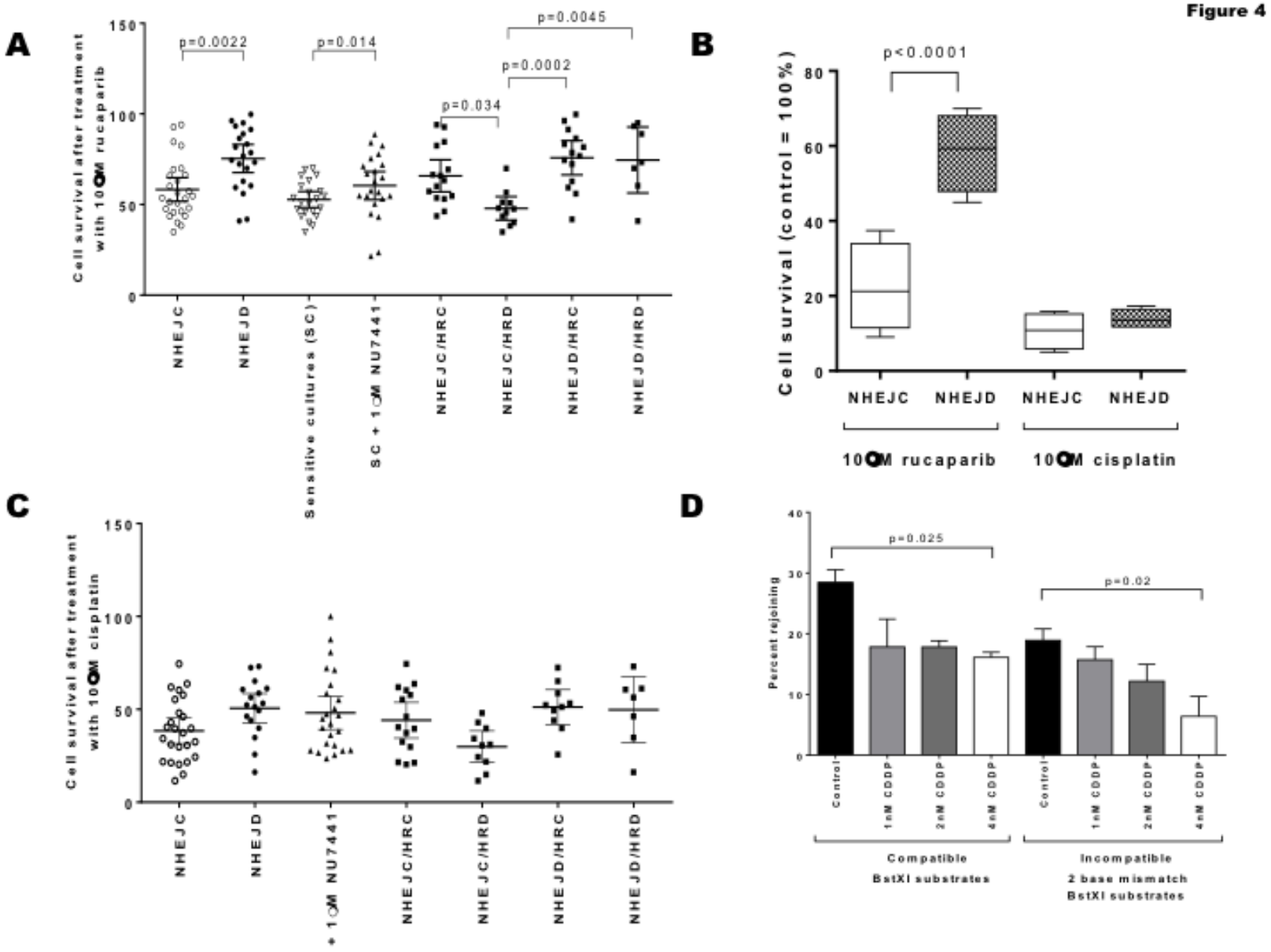
A
Cell survival after treatment with 10μM rucaparib
p=0.0022
p=0.014
p=0.034
p=0.0002
p=0.0045
NHEJC
NHEJD
Sensitive cultures (SC)
SC + 10μM NU7441
NHEJC/HRC
NHEJC/HRD
NHEJD/HRC
NHEJD/HRD
B
Cell survival (control = 100%)
p<0.0001
NHEJC
NHEJD
NHEJC
NHEJD
10μM rucaparib
10μM cisplatin
C
Cell survival after treatment with 10μM cisplatin
+ 10μM NU7441
D
Percent rejoining
p=0.025
p=0.02
Control
1nM CDDP
2nM CDDP
4nM CDDP
Compatible BstXI substrates
Incompatible 2 base mismatch BstXI substrates

Figure 5

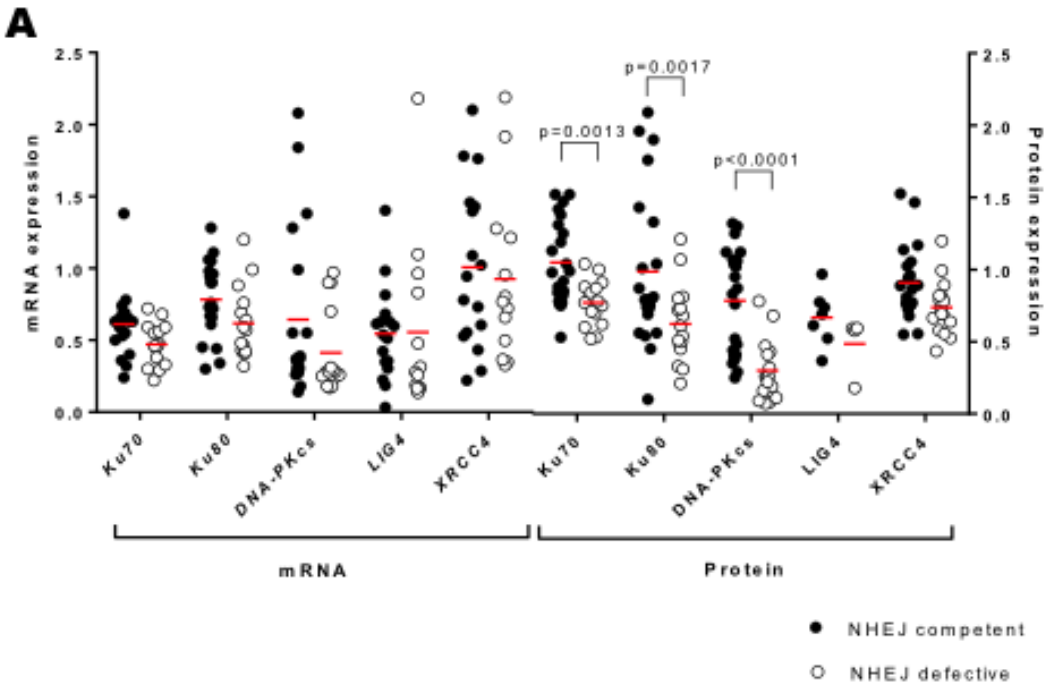
A
mRNA expression
Protein expression
2.5
2.0
1.5
1.0
0.5
0.0
p=0.0013
p=0.0017
p<0.0001
Ku70
Ku80
DNA-PKcs
LIG4
XRCC4
mRNA
Protein
NHEJ competent
NHEJ defective

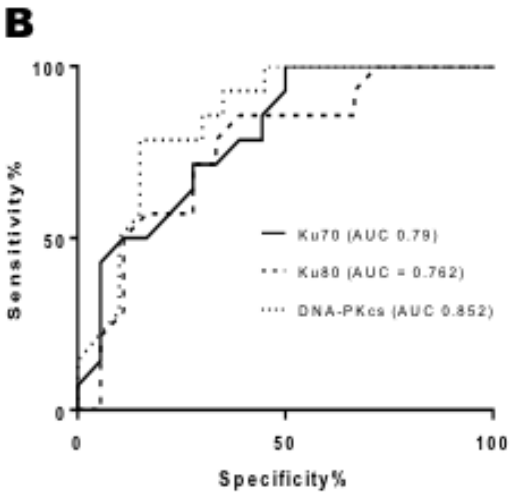
B
Sensitivity%
Specificity%
100
50
0
Ku70 (AUC 0.79)
Ku80 (AUC = 0.762)
DNA-PKcs (AUC 0.852)

Figure 6

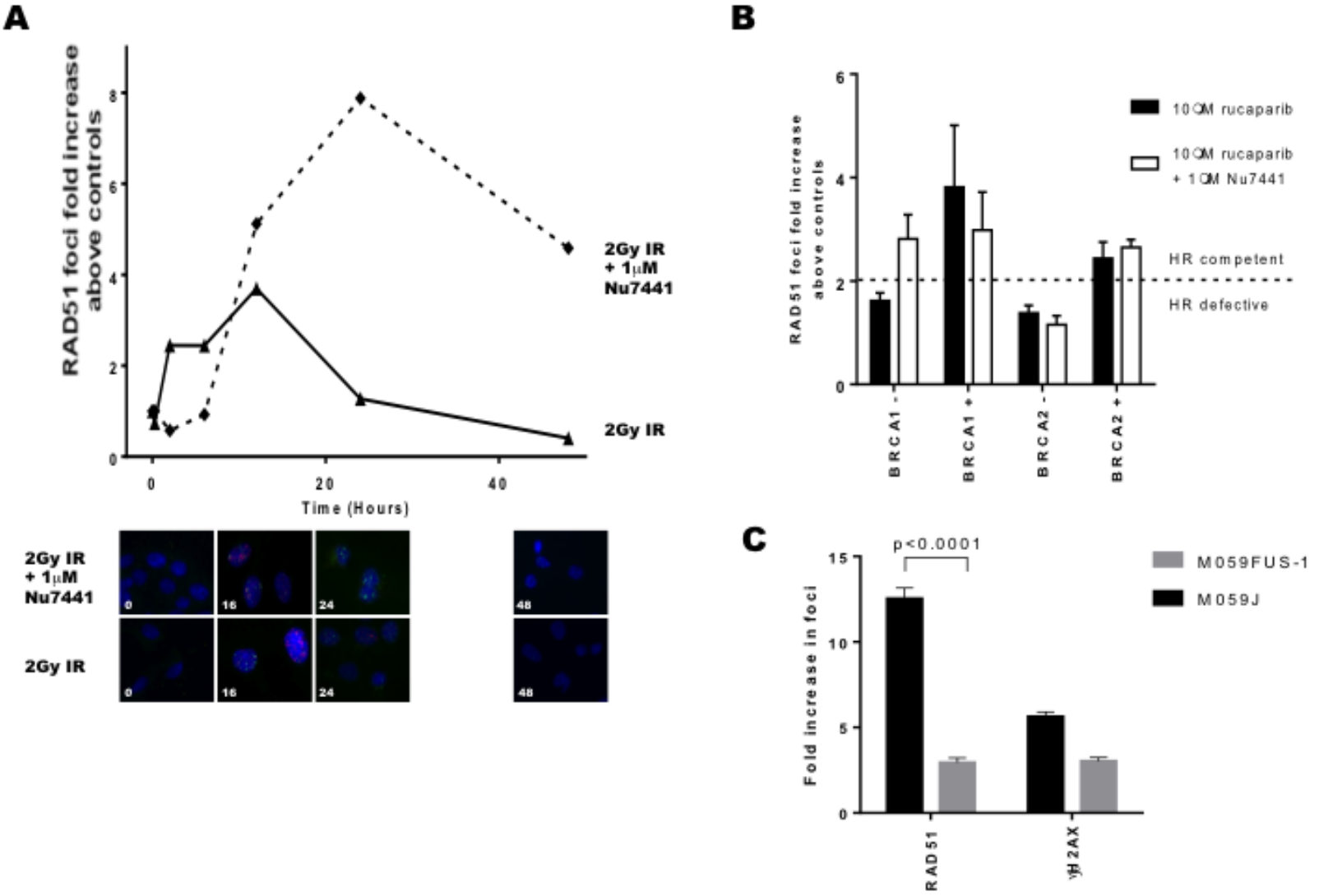
A
RAD51 foci fold increase above controls
Time (Hours)
2Gy IR + 1μM Nu7441
2Gy IR
2Gy IR + 1μM Nu7441
2Gy IR
B
RAD51 foci fold increase above controls
10 μM rucaparib
10 μM rucaparib + 1 μM Nu7441
HR competent
HR defective
BRCA1 -
BRCA1 +
BRCA2 -
BRCA2 +
C
p<0.0001
Fold increase in foci
M059FUS-1
M059J
RAD51
γH2AX

Figure 7

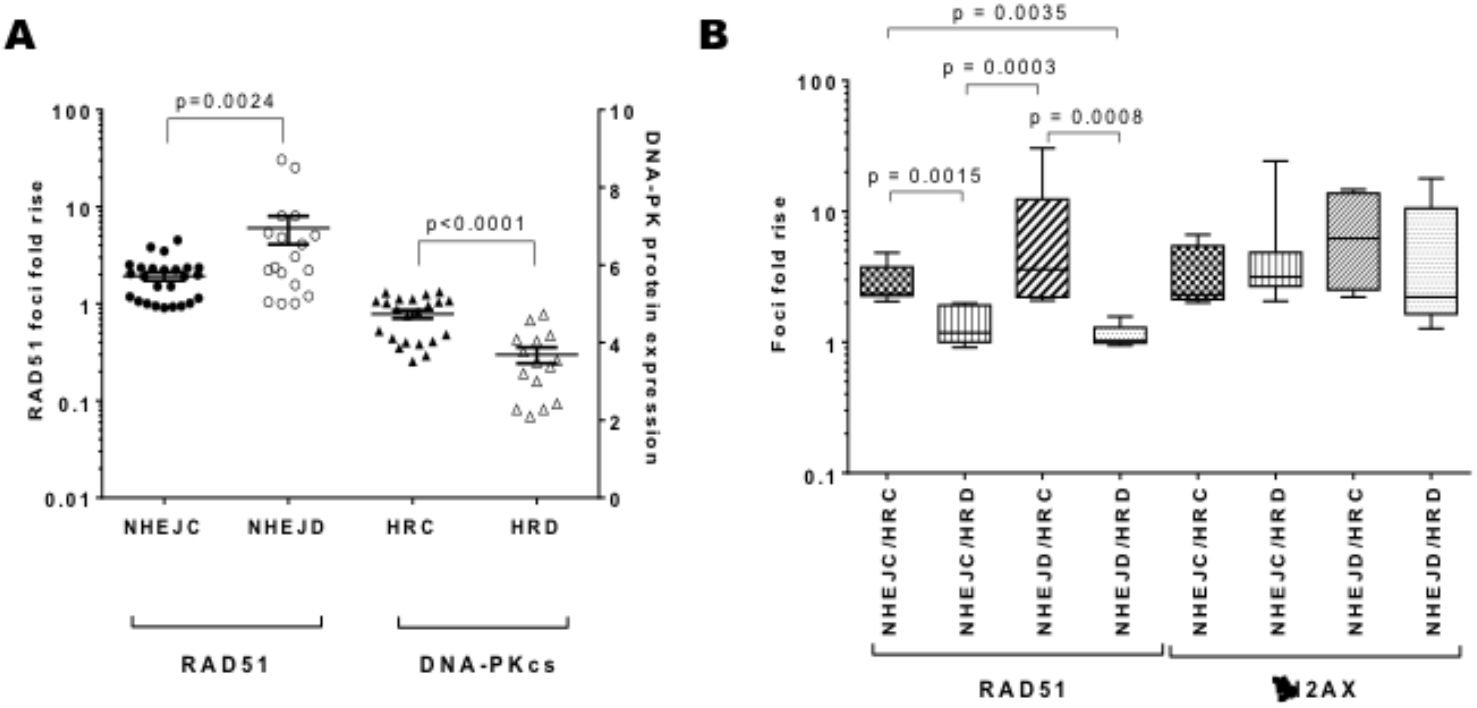
A
p=0.0024
p<0.0001
RAD51 foci fold rise
DNA-PK protein expression
100
10
1
0.1
0.01
10
8
6
4
2
0
NHEJC
NHEJD
HRC
HRD
RAD51
DNA-PKcs
B
p = 0.0035
p = 0.0003
p = 0.0008
p = 0.0015
Foci fold rise
100
10
1
0.1
NHEJC/HRC
NHEJC/HRD
NHEJD/HRC
NHEJD/HRD
NHEJC/HRC
NHEJC/HRD
NHEJD/HRC
NHEJD/HRD
RAD51
γH2AX